

# Amelioration of Penetrating Ballistic-Like Brain Injury Induced Cognitive Deficits after Neuronal Differentiation of Transplanted Human Neural Stem Cells

Markus S. Spurlock,<sup>1,\*</sup> Aminul I. Ahmed,<sup>1,\*</sup> Karla N. Rivera,<sup>1</sup> Shoji Yokobori,<sup>1</sup> Stephanie W. Lee,<sup>1</sup> Pingdewinde N. Sam,<sup>1</sup> Deborah A. Shear,<sup>2</sup> Michael P. Hefferan,<sup>3</sup> Thomas G. Hazel,<sup>3</sup> Karl K. Johe,<sup>3</sup> Shyam Gajavelli,<sup>1</sup> Frank C. Tortella,<sup>2</sup> and Ross M. Bullock<sup>1</sup>

## Abstract

Penetrating traumatic brain injury (PTBI) is one of the major cause of death and disability worldwide. Previous studies with penetrating ballistic-like brain injury (PBBi), a PTBI rat model revealed widespread perilesional neurodegeneration, similar to that seen in humans following gunshot wound to the head, which is unmitigated by any available therapies to date. Therefore, we evaluated human neural stem cell (hNSC) engraftment to putatively exploit the potential of cell therapy that has been seen in other central nervous system injury models. Toward this objective, green fluorescent protein (GFP) labeled hNSC (400,000 per animal) were transplanted in immunosuppressed Sprague–Dawley (SD), Fisher, and athymic (ATN) PBBi rats 1 week after injury. Tacrolimus (3 mg/kg 2 days prior to transplantation, then 1 mg/kg/day), methylprednisolone (10 mg/kg on the day of transplant, 1 mg/kg/week thereafter), and mycophenolate mofetil (30 mg/kg/day) for 7 days following transplantation were used to confer immunosuppression. Engraftment in SD and ATN was comparable at 8 weeks post-transplantation. Evaluation of hNSC differentiation and distribution revealed increased neuronal differentiation of transplanted cells with time. At 16 weeks post-transplantation, neither cell proliferation nor glial lineage markers were detected. Transplanted cell morphology was similar to that of neighboring host neurons, and there was relatively little migration of cells from the peritransplant site. By 16 weeks, GFP-positive processes extended both rostrocaudally and bilaterally into parenchyma, spreading along host white matter tracts, traversing the internal capsule, and extending ~13 mm caudally from transplantation site reaching into the brainstem. In a Morris water maze test at 8 weeks post-transplantation, animals with transplants had shorter latency to platform than vehicle-treated animals. However, weak injury-induced cognitive deficits in the control group at the delayed time point confounded benefits of durable engraftment and neuronal differentiation. Therefore, these results justify further studies to progress towards clinical translation of hNSC therapy for PTBI.

**Keywords:** behavior deficit; cell transplantation; hNSC; neuronal differentiation; PBBi; TBI

## Introduction

**T**RAUMATIC BRAIN INJURY (TBI) is a critical public health problem worldwide.<sup>1</sup> TBI involving firearm injury is an increasingly serious issue in the United States, costing > \$70–75 billion annually.<sup>2,3</sup> Timely neurosurgical intervention aided by improved neuroimaging and advances in acute trauma management have lowered the firearm fatality rate.<sup>4–6</sup> The proportion of gunshot wound survivors among disabled TBI patients has been rising steadily.<sup>7–12</sup> Among brain injuries, penetrating traumatic brain in-

juries (PTBI) are associated with the worst outcomes,<sup>13–15</sup> and no effective restorative treatment beyond physical therapy is currently available to mitigate post-TBI disability and associated cognitive deficits.<sup>16–18</sup> Therefore, there is an urgent need to explore additional treatment options to address long-term TBI-related disabilities.

Failure of injury-induced regenerative neurogenesis, chronic inflammation, and atrophy underlie poor outcomes.<sup>19–21</sup> Loss of neurons and consequent brain atrophy in TBI survivors<sup>22–25</sup> has been recapitulated in a survivable rat model: penetrating ballistic-

<sup>1</sup>Miami Project to Cure Paralysis, Miami, Florida.

<sup>2</sup>Branch of Brain Trauma Neuroprotection and Neurorestoration, Center for Military Psychiatry and Neuroscience, Walter Reed Army Institute of Research, Silver Spring, Maryland.

<sup>3</sup>Neuralstem, Inc. Germantown, Maryland.

\*The first two authors contributed equally.

like brain injury (PBBI)<sup>26–28</sup> Because of the extremely rapid cell loss following PBBI, acute neuroprotection alone has had limited success in mitigating damage.<sup>29,30</sup> Therefore, exploration of exogenous cell transplantation to aid recovery is necessary.

Human amniotic membrane placental stem cells (AMP) have been used in PBBI.<sup>26,31</sup> AMP secreted trophic factor releases significantly attenuated axonal degeneration.<sup>26,31,32</sup> Among the non-neural stem cells from which neural stem cells (NSC) have been derived, AMP have exhibited the best potential and ability to alleviate TBI-related cognitive deficits.<sup>33,34</sup> In contrast to few reports of mesenchyme-derived NSC integration,<sup>35–38</sup> neural precursors have been the subject of several successful studies.<sup>39–44</sup> Immunodeficient rodents or host immunosuppression with allografting<sup>45,46</sup> provide the best-case scenario for engraftment. Upon engraftment, xenografted NSC aid endogenous repair and behavior modification.<sup>47–50</sup> In contrast, first trimester (8–15 weeks) human fetal neural stem cells conferred only early, transient alleviation of TBI deficits.<sup>51–60</sup> In spite of xenotransplantation, there was no consensus on necessity or duration of immunosuppression<sup>59,61,62</sup> The resulting immunorejection hindered engraftment and long-term survival in rodent models of TBI.<sup>63</sup> Poor transient engraftment was marked by low neuronal differentiation of transplanted cells.<sup>52,55,64</sup> Such confounding data dampened enthusiasm for clinical translation. Only recently, to overcome these shortfalls, a novel TBI xenotransplantation model with athymic (ATN) rats was developed, and brain repair was tested with long-term ( $\geq 2$  months) human embryonic stem cell (hESC) derived NSC (hNSC) transplantation. Transplanted hNSC survived for at least 5 months post-transplantation and differentiated into mature neurons, astrocytes, and oligodendrocytes. The hNSC transplantation facilitated cognitive recovery without affecting either lesion volume or tissue volume.<sup>65</sup> Similar to rat NSC, an overall increase in host hippocampal neuron survival was observed.<sup>47,65</sup> The authors concluded that hNSC transplantation may be a viable, long-term therapy to restore cognition after brain injury.<sup>65</sup> The United States Food and Drug Administration (FDA) (Rockville, MD) recommends that evidence of cell fate post-administration is necessary to uncover the activity and safety profile of the investigational cell therapy product. This can be achieved by demonstration of robust durable engraftment.<sup>66,67</sup>

In the past decade, Neuralstem Inc. had developed NSI-566, an epigenetically expanded bank of NSC derived from the 8-week-old human fetal spinal cord, which is not on the federal moratorium list for funding.<sup>68</sup> These cells have been subject to extensive pre-clinical safety testing and characterization, by multiple independent laboratories with multiple immunosuppression regimens.<sup>69–76</sup> The cells are produced under Current Good Manufacturing Practice (CGMP) regulations enforced by the FDA, and have been recently tested in several animal models. The FDA has approved the use of these cells in amyotrophic lateral sclerosis (ALS) and chronic spinal cord injury clinical trials.

In this proof-of-concept study, we evaluated the aforementioned fetal spinal cord-derived human neural stem cell line (NSI-566) in three strains of rats subjected to PBBI, and assessed survival, differentiation, distribution, and long-term effect on injury-deficit.

## Methods

### Study design and animals

All animal procedures followed guidelines established by the National Institute of Health (NIH) Guide for the Care and Use of Laboratory Animals, Animal Research: Reporting of *In Vivo* Experiments (ARRIVE), and were approved by the Walter Reed

Army Institute of Research (WRAIR) and University of Miami's Institutional Animal Care and Use Committees. Animals were randomized to experimental groups. Surgical procedures were performed under aseptic conditions. To identify which rodent strain best supported xenotransplantation, Fisher 344 and Sprague–Dawley (SD) with unilateral PBBI were produced. SD and Fisher 344 animals served as test strains to establish efficacy of a chemical immunosuppression regimen. The ATN SD “nude” rats served as positive control, as they lack T-cell-mediated immunity (see Table 1 for animal use). All animals were acquired from Envigo (Indianapolis, IN) at 2–3 months of age, and were operated on at an initial weight of  $\geq 280$  g. Following establishment of the transplant paradigm, behavioral assessments were evaluated in a separate study with immunosuppressed SD rats. The sample size calculations are described in the subsequent behavior testing section. Digitizing behavioral data from recorded video tapes, green fluorescent protein (GFP) cell number quantitation in histological sections using unbiased stereology was performed by investigators blinded to the study design and experimental groups. They were also not involved in surgeries, behavior testing, or planning of the experiments.

### Anesthesia

Anesthesia was induced with isoflurane (2–5%) delivered in a mixture of 70% nitrogen and 30% oxygen. Body temperature was maintained at normothermia ( $37 \pm 1^\circ\text{C}$ ) throughout all surgical procedures by means of a homeothermic heating system (Harvard Apparatus, South Natick, MA).

### PBBI

The PBBI apparatus consists of a penetrating probe (Kadence Science, Lake Success, NY), a stereotaxic frame (Kopf, Tujunga, CA) equipped with a probe holder, and a hydraulic pressure-pulse generator (4B080; MITRE, MA). The penetrating probe is made of a 20G stainless steel tube with fixed perforations along one end that are sealed by a piece of airtight elastic tubing. The anesthetized rat was secured in a stereotaxic frame, and an incision was made along the midline to expose the dorsal surface of the skull. A cranial window was made at +4.5 mm anterior-posterior (AP) and +2mm medial-lateral (ML) from bregma on the right frontal pole. The multi-port balloon-tipped probe was inserted through the burr hole 12 mm into the brain at an angle 25 degrees lateral from midline and 50 degrees deep from the surface. The balloon was then rapidly expanded with water to 6.33 mm diameter for 40 ms by activating the HPD-1700 generator to induce a unilateral PBBI at 10% brain volume. This level of expansion produced a severe but survivable ( $< 10\%$  mortality) temporary cavity mimicking a ballistic shock-wave. The probe was retracted from the rat, the wound was closed with 9 mm wound clips, and the incision site was treated with topical antibiotic.<sup>77</sup>

### Cell transplantation

Transplants were performed 7–10 days following injury. This time point was selected based on the expected abatement of the initial injury-induced inflammatory response and the scheduled immunosuppression regimen, and to avoid freezing or prolonged storage of cells. The anesthetized rat was secured in a stereotaxic frame, and the scalp was reopened along the midline to expose the skull surface. A Hamilton 8000 Gastight 10  $\mu\text{L}$  micro syringe was backfilled and flushed with suspension media and then attached to a World Precision Instruments UMP3 micro syringe injector and micro4 controller. The syringe was filled with NSI-566 cells in suspension media (concentration of 100,000 cells/ $\mu\text{L}$ ).<sup>47</sup> A burr hole was made at  $-2.5$  mm AP and +3 mm ML from bregma, ipsilateral to the injury. The micro syringe was lined up at  $-2.5$  mm AP and +3 mm ML from bregma and advanced vertically 6 mm

TABLE 1. EXPERIMENTAL GROUPS, SAMPLE SIZE, AND FIGURES

Exp no.	Measurement	Experimental group	n/group	Results
1	Engraftment			
	Week 1 post-transplantation	Athymic SD PBBI+hNSC	1	
	Week 1 post-transplantation	SD PBBI+hNSC	2	Fig. 2
	Week 2 post-transplantation	Athymic SD PBBI+hNSC	1	
	Week 2 post-transplantation	SD PBBI+hNSC	2	Fig. 3
	Week 5 post-transplantation	Athymic SD PBBI+hNSC	1	
	Week 5 post-transplantation	SD PBBI+hNSC	2	Fig. 1
	Week 8 post-transplantation	Athymic SD PBBI+hNSC	7	
2	Week 8 post-transplantation	Fisher PBBI+hNSC	6	
	Week 8 post-transplantation	SD PBBI+hNSC	10	Figs. 1–3
	Morris Water Maze	SD-Sham	11	Fig. 7A and B
		SD-PBBI-Vehicle	9	
		SD-PBBI+hNSC	9 <sup>a</sup>	
	Week 8 post-transplantation	SD-PBBI+hNSC	6/9 <sup>a</sup>	Figs. 4 and 6
	Week 16 post-transplantation	SD-PBBI+hNSC	3/9 <sup>a</sup>	Figs. 1,3,4–6

<sup>a</sup>Three animals from this group were allowed to survive for 16 weeks post-transplantation histology.

The first column lists the major experiment. The subsequent columns lists outcome measured, experimental groups, and number of rats per group, and in which figures the results are presented.

PBBI, penetrating ballistic-like brain injury; hNSC, human neural stem cell.

deep into the brain. Using the micro pump preset, 2 μL were injected at a rate of 1 μL/min. The needle was then retracted to 4 mm depth from the brain surface, and another 2 μL were injected. The transplant locations were within the perilesional zone (PLZ) of the injury, adjacent to the primary injury cavity. This PLZ was previously determined by autoradiographically mapping regional metabolic disruption and secondary cell death in this region following injury.<sup>78</sup>

**Immune suppression**

Tacrolimus was administered intraperitoneally (i.p.) at 3 mg/kg beginning 2 days prior to transplantation and continued daily for 2 weeks, then switched to 1 mg/kg/day for the rest of the survival period. Methylprednisolone was injected i.p. weekly beginning on the day of transplant at 10 mg/kg, continuing thereafter at 1 mg/kg throughout the course of survival. Mycophenolate mofetil in 5% dextrose was injected i.p. 30 mg/kg daily, only for the 1st week following transplantation.<sup>71,79,80</sup> The animals were maintained on a 12 h/12 h light/dark cycle and given food *ad libitum*. They were provided an enhanced recovery diet following surgical procedures until baseline weight was re-established. Immune-deficient animals were handled under a laminar airflow hood, in a dedicated closed vivarium room, with sterile gloves for all long-term care procedures.

**Behavior testing with the Morris water maze (MWM) test**

Sample size calculations for behavioral outcome in this model were computed *a priori* with software “G\*Power 3.1” with type I error α set at 0.05 with power (1-type II error β) 0.8 and estimated effect size (Cohen’s *d*) *d* = 0.66.<sup>77</sup> Learning and memory were assessed at 8 weeks following transplant using the MWM with video tracking system. A platform was placed in a pool (75 cm deep; 175 cm diameter filled to a depth of 60 cm with water maintained at temperature of 22°C) just under the water level at a fixed location 35 cm from the wall of the pool in the northeast quadrant. For each trial, the rat was released into the pool facing the wall from north, south, east, or west starting positions. The north and east start positions were designated short arms and the south and west positions were designated long arms. Start position of each trial was semi-random, alternating short and long, with each start point used once

daily. Once released, the rat was allowed to swim until it reached the platform, or until a period of 60 sec had elapsed. If the rat failed to reach the target in the given period, it was manually placed on the platform. Once on the platform, the rat was allowed 10 sec rest before being returned to the cage for a 4–5 min inter-trial rest. Four trials (one at each start position) were performed daily over the course of the first 4 days. Latency to platform presented as the mean ± standard deviation in contrast to previously used methods with the TBI, PBBI models with cell transplantation, where the deficit persisted at least 10 weeks following injury.<sup>47,65,77,81</sup> The EthoVision Video Tracking Software (Noldus EthoVision XT) was used to confirm latency to reach platform (which was manually recorded with a stopwatch immediately after the trial); path length and swim speed were traced from video using EthoVision. Animals with evidence of far greater than average transplant rejection (criteria such as surviving transplant cell counts at 8 weeks below one third of average cell survival, and the presence of immune cells) were excluded from behavior analyses.

**Specimen collection and histology**

Rats were perfused transcardially with 0.1M phosphate-buffered saline (PBS), followed by cold 4% paraformaldehyde (PFA) in 0.1M phosphate buffer. Brains were dissected out and post-fixed in 4% PFA for 12 h, then transferred to a 30% sucrose solution for 24 h. Brains were frozen in M-1 embedding matrix using dry ice, and stored at –20°C before being sectioned on a cryostat at 40 μm thickness. Sections were stored free floating in 0.02% sodium azide in PBS prior to immunohistochemistry. Samples were assessed with the following primary antibodies: anti-GFP (Millipore MAB1083), NeuN (Millipore MAB377), doublecortin (DCX) (Millipore AB2253), glial fibrillary acidic protein (GFAP) (Dako Z0334), Olig2 (Millipore AB9610), HuNu (Millipore MAB1281), Ki67 (Millipore AB9260), nestin (Millipore ABD60), MBP (Covance, SMI 94), and Calbindin (Cell Signaling #2136X). Appropriate fluorescent secondary antibodies were used (Life Technologies) with 2-(4-amidinophenyl)-1H-indole-6-carboxamide (DAPI) prior to mounting and imaging.

**Imaging and analysis**

Volumetric GFP cell counts were generated using the physical fractionator method in StereoInvestigator (version 10.6 Stereo

Investigator, MBF Bioscience, Williston, VT) on evenly spaced (0.2 mm apart) brain sections, and used to calculate estimated total cell survival. The percentage of NeuN and GFP double-positive cells in grafts was determined by analysis of raw image files with Imaris 6.0.0.1 software. High-resolution fluorescent images were generated on a confocal microscope ( $n=3-5$  sections/brain; 3 brains/group). Using Imaris analysis software (version 8.0.1), and based on NeuN-positive host hippocampal neurons, the fluorescence intensity and object diameter were estimated. This served as the threshold for NeuN signal; similarly, a GFP limit was set using the transplanted cells. Points of NeuN-positive signal were automatically counted by approximate diameter and intensity based on host neurons (using the Spots tool). Similarly, GFP-positive points were counted based on diameter and relative background subtraction. The co-occurrence of both signals as calculated by the Imaris software was used to estimate NeuN positivity of grafts at 8 and 16 week time points. The synaptophysin signal was similarly analyzed in Imaris by comparing the occurrence of synaptophysin-positive spots at a set signal threshold in sample sites from transplant location versus contralateral regions of host brain expressing no GFP signal. The incidence of synaptophysin signal was compared overall between GFP-negative and GFP-positive tissue.

### Statistical analysis

Histopathological and behavioral end-points were compared by independent samples *t* tests or analysis of variance (ANOVA) followed by Fisher protected least significant difference (PLSD) post-hoc and paired *t* test analyses when appropriate (SigmaStat). All data are presented as the mean  $\pm$  standard deviation, and *p* values  $<0.05$  were considered significant.<sup>77,82</sup> For all experiments, the trained investigators performing the behavioral and neuropathological assessments were blinded to the experimental groups. MWM results were compared using two way repeated measures ANOVA followed by Tukey's test. Data were graphed using GraphPad version 6.0.

## Results

### Survival

Following PBBI expansion,  $\sim 6$ mm lesion is produced, spanning the dorsal frontal cortex (+3.0 mm Bregma), anterior striatum, anterior-lateral edge of the caudate nucleus, corpus callosum, and anterior caudate-putamen, and terminating near the amygdala ( $-3.0$  mm Bregma). The injury core and PLZ release a host of inflammatory cytokines including IL-1 $\beta$ , and thus contribute to secondary injury propagation.<sup>28,83</sup> It was not known to what extent the toxic PBBI milieu would impede survival of a human cell transplant. Therefore, the human NSI-566 NSCs were transplanted into three different rat strains subjected to PBBI: 1) outbred SD standard laboratory rats, 2) relatively less immunocompetent Fischer 344 rats, and 3) immunocompromised SD ATN rats. The SD and Fischer animals were treated with an immunosuppression regimen as per the protocol previously described.<sup>71,79,80</sup> ATN rats were treated with only methylprednisolone weekly, to reduce injury-induced inflammation. Rats were euthanized at specific time points to track graft survival (1, 5, 8, and 16 weeks following transplantation). Robust engraftment could be seen as far as 16 weeks post-transplantation, the last time point tested. In the first set of experiments, at 8 weeks, grafts were present in 15/16 SDs, 9/10 ATNs, and 4/6 Fischer 344 (28/32 total). The number of GFP-positive cells was quantitated using unbiased stereological counting, and supplemented with manual counts of confocal images when necessary. No significant difference between ATN and immunosuppressed SD or Fischer rats with PBBI was found in the

number of surviving graft cells, which averaged 150% of the original transplanted cell numbers (SD =  $6.5 \times 10^5$ , ATN =  $6.2 \times 10^5$ , Fischer =  $5.7 \times 10^5$  cells). In next set of experiments for behavioral analysis, following stable immunosuppression of SD rats  $3.7 \times 10^5 \pm 1.1 \times 10^5$  cells could be counted at 8 weeks post-transplantation. This suggests that the immunosuppression regimen is effective in supporting xenogeneic human cell graft survival for the majority of the animals (9/12), in the rodent PBBI model. The transplant size did not vary between 5 and 16 weeks post-transplantation (Fig. 1).

### Differentiation

The following results were produced in immunosuppressed SD rats. The human origin of the GFP-positive xenograft was confirmed with HuNu, a marker for human cell nuclei (Fig. 2B, E, and H). At 1 week post-transplant, the cells appeared rounded, undifferentiated, and  $<5 \mu\text{m}$  in diameter (Fig. 2A–C). By 8 weeks, the cells had hypertrophied to  $>10 \mu\text{m}$  across with extended neuronal-like processes (Fig. 2D–I). Processes extending from the central soma spread out into the host tissue, lending support to the development of multipolar neurons. The process of transplanted NSC differentiation was evident based on the decreasing nestin-immunoreactivity over time. Nestin expression was high in transplanted cells at 2 weeks, but reduced by 8 weeks, and was almost absent by 16 weeks (Fig. 3A–L). A similar pattern was observed with nuclear Ki67, where expression at 2 weeks had diminished by 16 weeks (Fig. 3M–T). In brain sections ( $\sim -4.0$  mm bregma, 1 mm caudal to lesion) from a representative immunosuppressed SD rat shown in Figure 4A, The DAPI-stained nucleus (Fig. 4B) indicated by a white arrow belongs to transplanted GFP-positive cells (Fig. 4C) that expressed the immature neuronal lineage marker DCX at 8 weeks (Fig. 4D). A  $27 \pm 12\%$  fraction of GFP+ cells also expressed NeuN, a marker for mature neurons (1729 NeuN<sup>+</sup> out of 6489 GFP+ cells) (Fig. 4E). The combined fluorescence of GFP and DCX (Fig. 4F) dilutes the GFP intensity (compare C with F). Overlay of DCX and NeuN (Fig. 4G) shows different localization of the two antigens. The cell appears yellow (Fig. 4H) because of the combined fluorescence of GFP and NeuN. Corresponding images for the 16 week post-transplantation time point show diffuse DCX expression because of the greater fragmentation into number of processes (Fig. 4D'). At this time, the fraction of NeuN-immunoreactivity of GFP+ cells increased to  $43 \pm 17\%$  (2791 NeuN<sup>+</sup> out of 6357 GFP+ cells), indicating prolonged neuronal differentiation (Fig. 4H'). Overlays confirm the co-expression of DCX with GFP (Fig. 4F') and NeuN with GFP (Fig. 4H'), and lowered DCX in NeuN cells (Fig. 4G') (compare G with G'). Further, by week 16 post-transplantation, Calbindin immunoreactivity could be observed in transplant-derived cells with neuronal morphology (Fig. 4I–K and 4I'–K'). Robust expression of presynaptic protein synaptophysin could be seen in the transplant compared with the host (Fig. 4L), whereas there was no difference in the expression of the postsynaptic protein gephyrin (data not shown). Quantitative analysis of synaptophysin expression in GFP+ tissue and in contralateral GFP- host tissue indicated a significant increase in expression at the site of transplantation. (GFP+ synaptophysin =  $350.6 \pm 20.7$  puncta/mm<sup>2</sup>  $n=8$ , GFP- synaptophysin =  $251.4 \pm 21.9$  puncta/mm<sup>2</sup>  $n=9$ ;  $p=0.005$ ) (Fig. 4M). Further orthogonal analysis confirmed transplant-derived synaptophysin *via* demonstration of fluorescence overlap (Fig. 4N–P).

The transplant cells did not express GFAP, a marker for astrocytes (Fig. 5A–C), or Olig2, a marker for oligodendrocytes as the

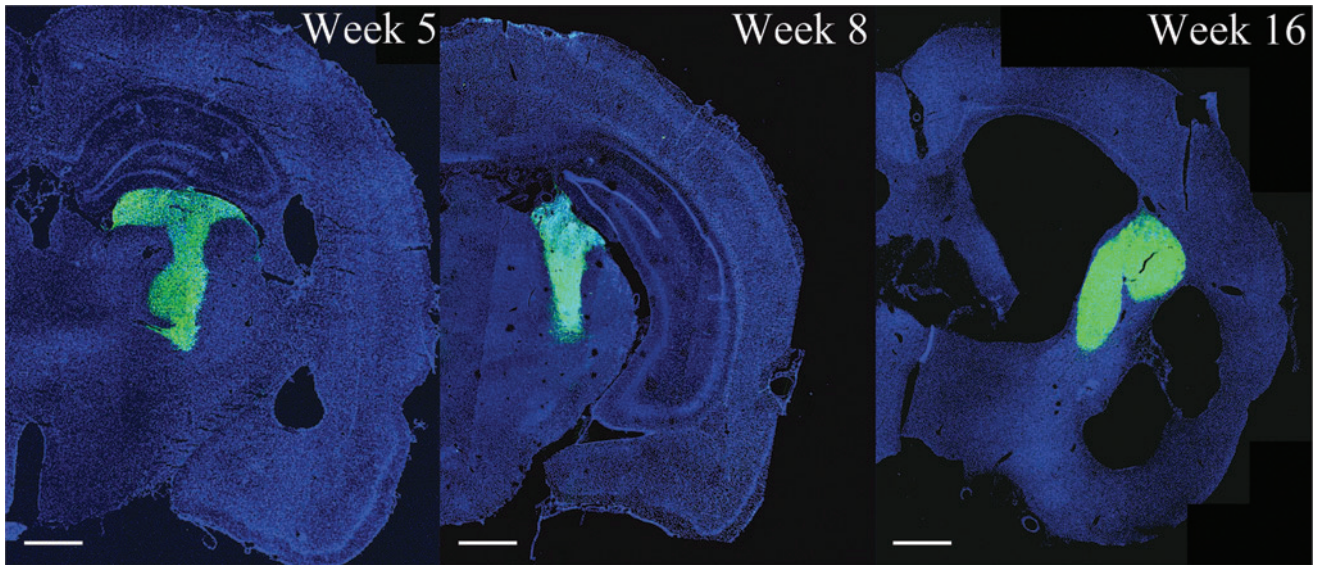


**FIG. 1.** Representative brain sections containing green fluorescent protein (GFP) human neural stem cell grafts (hNSCs) at 5, 8, and 16 weeks post-transplantation in immunosuppressed Sprague–Dawley (SD) rats with penetrating ballistic-like brain injury (PBBi). Adjacent to PBBi lesion, persistent engraftment (GFP fluorescence) of hNSCs with little migration from transplant site is evident. Scale bar 1 mm.

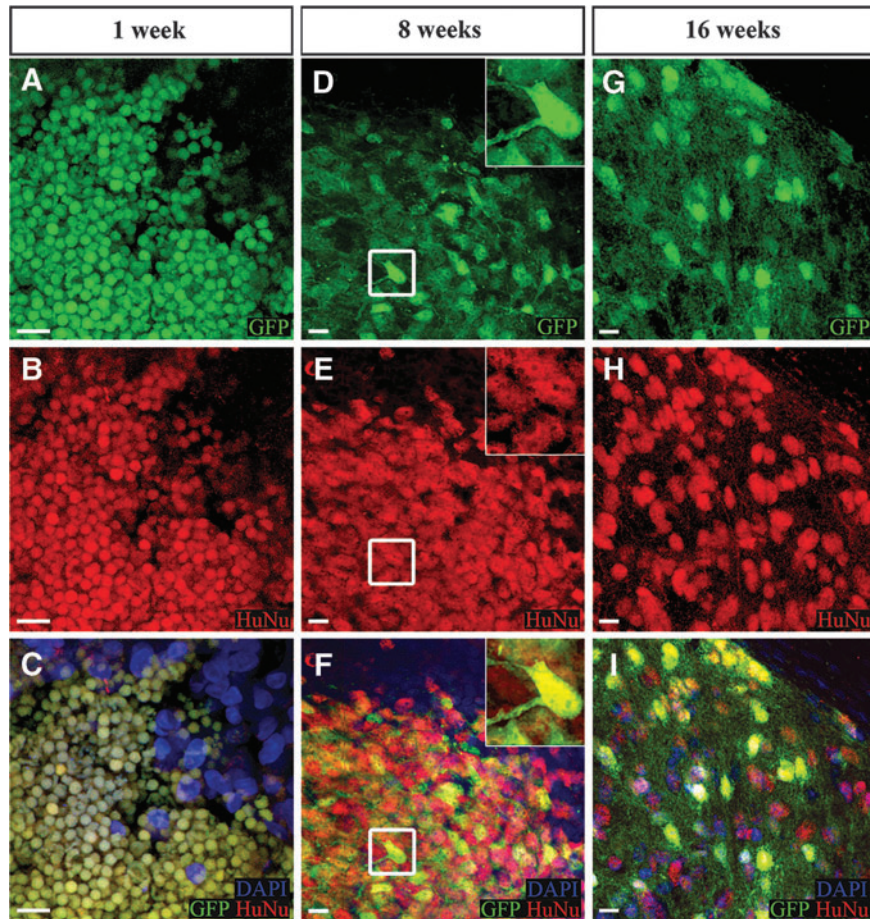


**FIG. 2.** Morphological changes with time *in vivo* of human neural stem cell (hNSC)-green fluorescent protein (GFP). At 1 week post-transplantation, cells exhibit round undifferentiated neural stem cell morphology devoid of processes (A). HuNu immunoreactivity (red) confirms human origin of cells (B). Fluorescence overlay of GFP with HuNu renders hNSC yellow, which is absent in the host (top right corner of C). By week 8, GFP cells have differentiated neural cellular morphology (D–F). The cell in the white square at a higher magnification (insets). The morphology persists at week 16 (G–I). Scale bar 10  $\mu$ m.

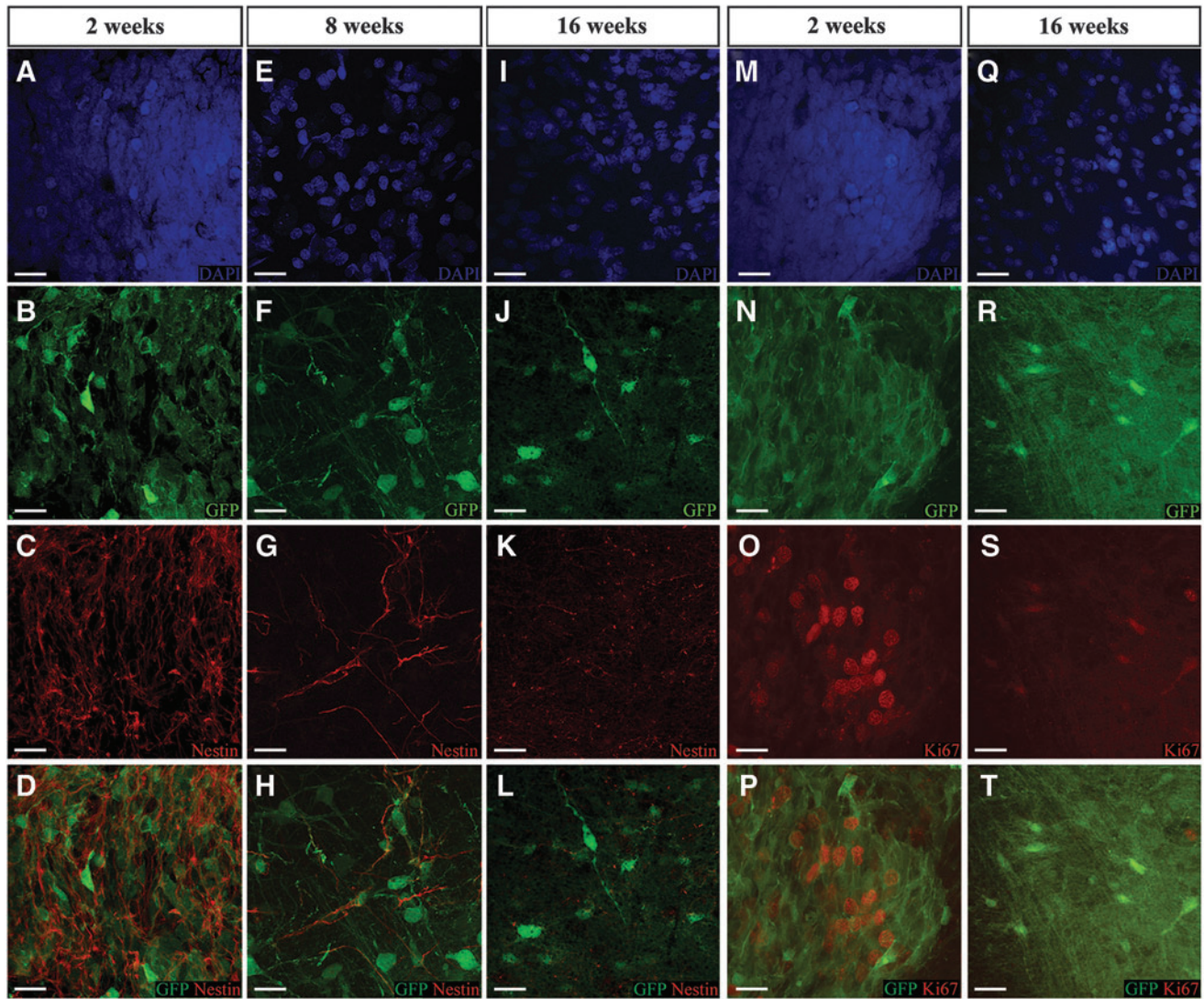


**FIG. 3.** DAPI fluorescence reflects the nuclear density at time points indicated above the image (A, E, I, M, D, Q). GFP fluorescence is also relatively similar (B, F, J, N, R) while immunoreactivity to Nestin, neural stem cell marker (red) is diminished over time (C, G, K), similarly anti-Ki67 immunoreactivity diminished with time (O, S). The bottom panel shows the combined fluorescence of GFP and Nestin (D, H, L) or GFP and Ki67 (P, T). (Scale bar 10  $\mu$ m.)

human ubiquitin C promoter-driven GFP signal did not overlap with that from antibodies (Fig. 5D–F), as determined by evaluation of confocal imaging of transplant sites. Further, the GFP processes extending from the transplanted cells did not overlap with myelin basic protein from the host, indicating lack of transplant-derived myelination even at 16 weeks (Fig. 5G–I).

#### Distribution

The GFP cell bodies could be seen up to 1 mm from the initial transplant sites at 8 weeks and even at 16 weeks, indicating little migration of the cells from injection sites. Cells extended processes up to  $\sim$ 0.5–1 mm from the site of transplantation, by 8 weeks, and those on the edges of the site extended these processes farther into host tissue. The transplant-derived processes, however, extended 5 mm rostral and 13 mm caudal to transplant site. Transplanted cells could be seen all along the injection tracts in the thalamus, cortex, and hippocampus and bordering the lateral ventricle. Examples of transplant cell morphology were consistent with pyra-

midal cells in the cortex (Fig. 6A), hippocampus (Fig. 6B), and both bipolar and multipolar interneuron-like cells in the thalamus (Fig. 6C). This suggests that transplant cells responded to regional cues to determine differentiation patterns. Distally, processes were seen in the ventral brainstem into the spinal cord, extending over 13 mm from the primary transplant site (Fig. 6D–H). These GFP processes extended around the ipsilateral thalamus into the internal capsule (Fig. 6D, L, and N), along host white matter tracts, crossing the midline (Fig. 6J) and periaqueductal gray (Fig. 6M), and emerged along the contralateral white matter tracts (Fig. 6L and N). Shorter processes were observed throughout the cortex and parts of the hippocampus from the transplant tract.

#### Behavior

Significant impairment of spatial memory in SD rats with PBBI has been reported previously.<sup>77</sup> The effect of transplants on the PBBI-induced deficit was assessed using the MWM at 8 weeks post-transplantation. This time point was deemed the minimum

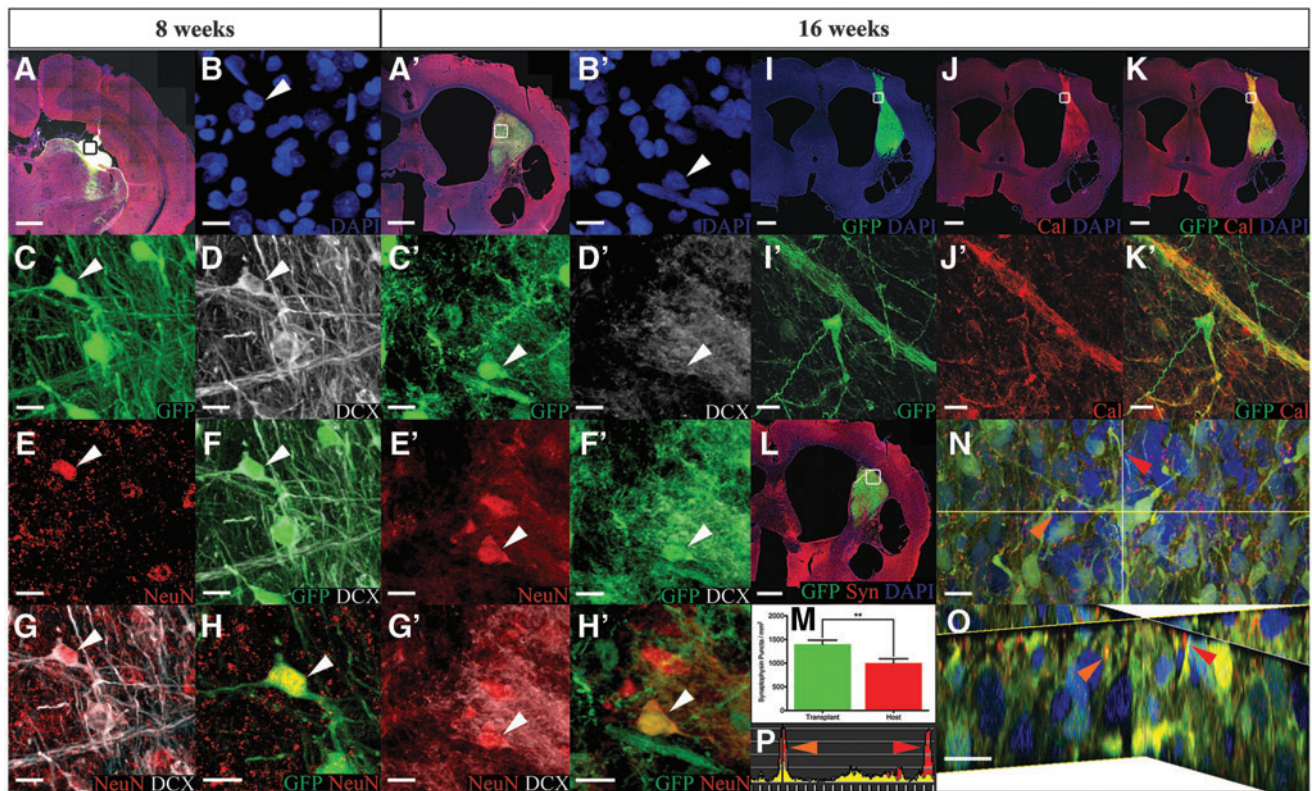


**FIG. 4.** Increasing neuronal differentiation of green fluorescent protein (GFP) human neural stem cell grafts (hNSCs) with time *in vivo* is evident from 8 week images (A–H) and corresponding 16 week images (A’–H’), in A, the image of the whole hemisphere at 8 weeks post-transplantation shows overlap of 2-(4-amidinophenyl)-1H-indole-6-carboxamide (DAPI), GFP, doublecortin (DCX), and NeuN fluorescence. The black square in A is shown at a higher magnification in B–H. The DAPI-stained nucleus indicated by a white arrow in B is GFP (C), strongly DCX<sup>+</sup> (D) with weak NeuN immunoreactivity (E). Overlay of GFP with DCX (F), DCX with NeuN (G), and GFP with NeuN (H) confirms neuronal differentiation of transplanted hNSC. Corresponding 16 week images (A’–H’) show weak, diffuse DCX (D’) and stronger NeuN (E’) that is confirmed by fluorescence overlay (F’–H’). Scale bar 10  $\mu$ m. Neuronal marker expression at 16 weeks. Transplant-derived neurons show immunoreactivity to a mature neuronal marker, Calbindin (I–K). DAPI-stained whole hemisphere image shows GFP transplant (I) that is Calbindin positive (Cal<sup>+</sup>) (J). Overlay renders transplant yellow (K). Scale bar 1 mm. The white square (in I–K) near the corpus callosum is shown at a higher magnification to highlight a single GFP cell bearing neuronal morphology that is Cal<sup>+</sup> (I’–K’). Scale bar 10  $\mu$ m. DAPI and anti-synaptophysin antibody stained whole hemisphere with 16 week transplant shows synaptophysin immunoreactivity in gray matter and transplant but not white matter (L). Quantitation of synaptophysin immunoreactivity (red puncta in L) revealed greater synaptophysin puncta in transplant (green) than in host (red) (M). The region in the white box is shown at a higher magnification as an orthogonal view with two representative synaptophysin puncta, one each for transplant (orange arrow) and host (red arrow) (N). A zoomed-in view shows the presence of GFP signal in transplant (orange arrow) but not host (red arrow) synaptophysin puncta. Quantitation of fluorescence is shown in P. Scale bar 10  $\mu$ m. The scale bar for A, A’, and I–L is 1  $\mu$ m.

duration needed for differentiation and integration of human neural stem cells.<sup>2,79</sup> For latency to platform, a two way repeated measures ANOVA (one factor repetition) revealed a statistically significant interaction between groups and acquisition days ( $F_{2,84}=2.689$ ,  $p=0.019$ ). Experimental groups were sham (no PBBI, no cells,  $n=12$ ), vehicle (PBBI, no cells,  $n=11$ ), and transplant (PBBI, cell transplant,  $n=9$ ). The main effect was with acquisition days ( $F_{2,84}=34.505$ ,  $p\leq 0.001$ ) but not experimental groups ( $F_{2,84}=1.861$ ,  $p=0.174$ ). Next all pairwise multiple comparison procedures (Tukey test) showed that latency to platform was reduced significantly in all experimental groups from day 1 to day 4 of testing (sham  $p<0.001$ , vehicle  $p=0.011$ , transplant  $p<0.001$ ). This decrease in latency to platform was not uniform in all groups (sham=63%, vehicle=33%, and transplant=72%). It plateaued from acquisition day 2 to day 4 in the vehicle group (PBBI+vehicle) while continuing to decline in both the sham and transplant groups (sham  $p=0.011$ , vehicle  $p=0.259$ , transplant  $p<0.001$ ). Latency was not significantly different between

sham and treatment groups ( $p=0.676$ ) (Fig. 7A). However, a one way ANOVA conducted on the day 4 data revealed significant between-group differences ( $F_{2,30}=5.952$  and  $p=0.0067$ ), with post-hoc analysis showing significant improvement on latency to the hidden platform versus PBBI+vehicle (Fig. 7B). The effect size (Hedge’s *g*) for latency to platform at 8 weeks post-transplantation was  $-1.33$  for PBBI+vehicle versus sham, whereas that for PBBI+vehicle versus PBBI+transplant was  $-1.0$ .

For path length, with experimental groups sham (no PBBI, no cells,  $n=12$ ), vehicle (PBBI, no cells,  $n=10$ ), and transplant (PBBI, cell transplant,  $n=9$ ), two way repeated measures ANOVA (one factor repetition) did not reveal a statistically significant interaction between groups and acquisition days ( $F_{2,81}=2.022$ ,  $p=0.072$ ). Albeit, the main effect was with acquisition days ( $F_{2,81}=20.319$ ,  $p\leq 0.001$ ) but not experimental groups ( $F_{2,81}=1.736$ ,  $p=0.195$ ) (Fig. 7C). One way ANOVA of the day 4 path length was also significant ( $F_{2,28}=6.791$  and  $p=0.0039$ ) (Fig. 7D). The path length

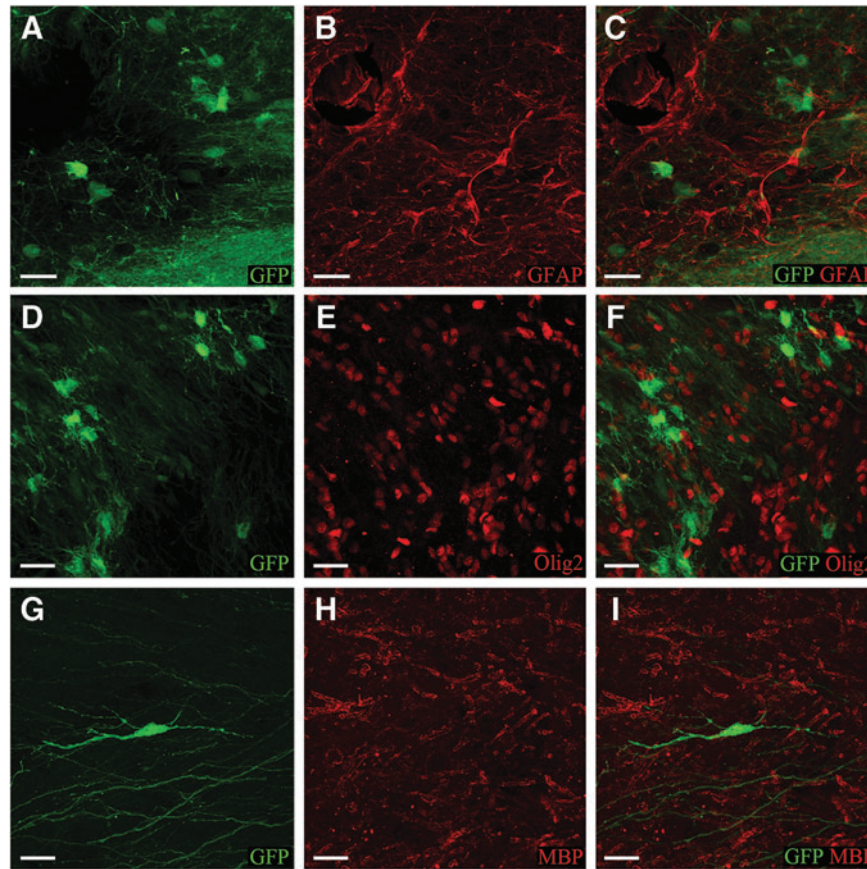


**FIG. 5.** The first, second, and third columns show GFP (A, D, G), antibody (B, E, H) and combined fluorescence (C, F, I) signal respectively. At 16 weeks post-transplantation, transplant cells do not express astrocytic marker, GFAP as evident by absence of overlap between GFP and GFAP (red) fluorescence (C). GFP positive transplant cells do not express oligodendrocytic precursor marker, Olig2 (F) or mature oligodendrocyte marker myelin basic protein (MBP) (I). (Scale bar 10  $\mu$ m.)

tracings of a representative animal of each group from four release points are shown in Figure 7E. The differences in swim speeds were not statistically significant (data not shown).

## Discussion

This study shows human fetal NSC survival, engraftment, and associated functional outcome at 8 weeks post-transplantation following PBBI in rats. This report of durable engraftment of CGMP hNSCs with coincident amelioration of TBI-induced behavioral deficit extends the pioneering efforts exploring the use of human fetal neural cells for TBI.<sup>59,64</sup> These results are comparable to previous studies in uninjured or TBI rodent models.<sup>45,46,59,64,84,85</sup> Further, we have shown survival with evidence of neuronal differentiation as far out as 4 months, thus meeting the criteria for durability.<sup>84</sup> The findings reported here are consistent with those on human fetal neural cell transplants in central nervous system (CNS) injury by Wu's<sup>52</sup> and Tuszynski's<sup>72</sup> groups. In both studies, engrafted hNSC in injured CNS projected over long distances covering almost the entire neuraxis,<sup>72,86</sup> and in particular, the fetal spinal cord-derived NSI-566 cells used in this study have been shown to support functional recovery after spinal cord injury.<sup>72</sup> It is a common trend to report the cell counts as percentage survival without direct evidence of lineage. The cells present at latter time points have not conclusively been shown to be the same at the time of transplantation. Therefore, we report quantitation of cells at the time point rather than

percentage of transplanted cell survival. The NSI-566 cell transplant morphology and neuronal antibody reactivity of the transplanted cells at 8 and 16 weeks suggests robust neuronal differentiation of transplanted NSCs in PBBI. The number of transplant-derived neurons reported in this study (43%) is much higher than that reported (1%) in other studies,<sup>59,64</sup> which could in part be the result of differences in immunosuppression protocol.<sup>71,79</sup> The combination of agents is critical for engraftment; previous studies showed complete rejection when only one agent was used.<sup>71,79,80</sup>

The protocol used in this study renders the animals as immunocompromised as ATN; therefore, the numbers reported here bear similarity to those with TBI ATN, in which ~38% of the transplanted cells expressed NeuN.<sup>65</sup> The duration of differentiation of hNSCs into NeuN-positive cells is consistent with a published report that showed that ~6–8 weeks were sufficient to induce transplant-derived neurogenesis.<sup>2,79,85</sup> The length of processes derived from hNSCs as a function of time is similar to that reported in the literature.<sup>59,85</sup> The lack of astrocyte or oligodendrocyte markers is consistent with previous reports at 12 weeks post-transplantation in TBI rats,<sup>59,64</sup> and could in part be the result of the short duration of the experiment (16 weeks). Human glial differentiation may occur at a slower rate following transplantation in rodents.

This conclusion is supported by the observation that in the spinal cord injury model, rat NSCs gave rise to 27% neurons and the rest glia, whereas fetal hNSC (NSI-566RSC) gave rise to 57% neurons with no gliogenesis 7 weeks post-transplantation,<sup>72</sup> although with



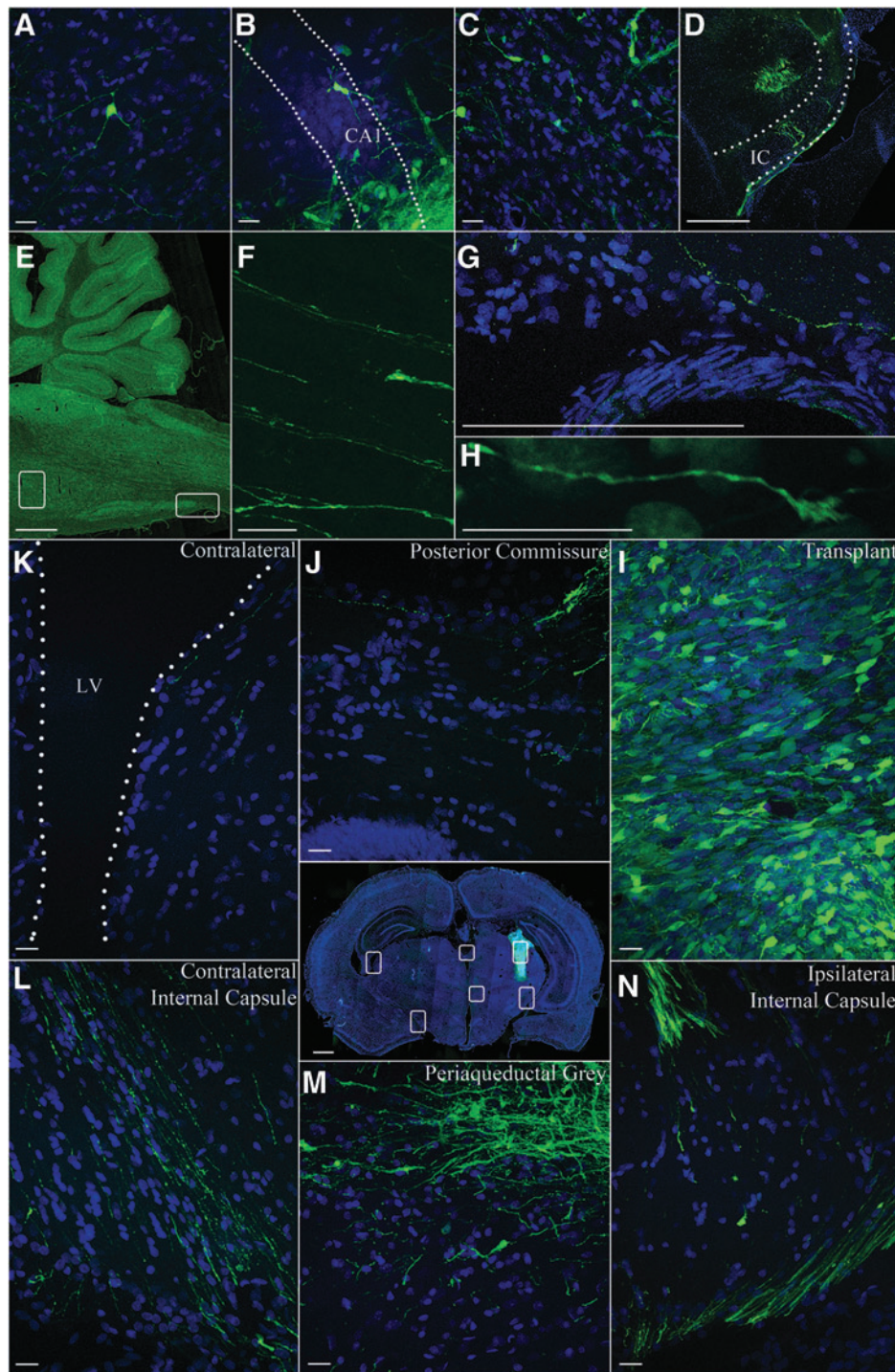


**FIG. 6.** Distribution of green fluorescent protein (GFP) cells and processes. Examples of transplant-derived cells and processes in the host parenchyma. Pyramidal-shaped cell in the cortex (A), hippocampus cornus ammonis 1 (CA1) (B), and thalamus (C) revealed by GFP and 2-(4-amidinophenyl)-1H-indole-6-carboxamide (DAPI) (blue) fluorescence. Cells in the thalamus appear to extend processes along the white matter tracts of the internal capsule (IC) (dotted outline in D). A sagittal section shows the brainstem and cerebellum in E. Higher resolution image of the boxes F and G show the presence of GFP fibers in the corresponding higher resolution image on the right. The tip of a GFP process with a growth cone morphology is shown in H.  $\mu\text{m}$  bar is  $10\ \mu\text{m}$  for A–C,  $1000\ \mu\text{m}$  for D, and  $10\ \mu\text{m}$  for F–H. Confocal image of penetrating ballistic-like brain injury (PBBI) brain section with GFP+ human neural stem cell grafts (NSCs) at week 8 post-plantation shows the distribution of transplant and GFP processes (image at center). White boxes in the image are shown at a higher magnification in a counterclockwise arrangement. The GFP+ transplant-derived processes bilaterally wrap the thalamus. GFP processes from the transplant (I) cross the posterior commissure (J) contralateral thalamic surface (contralateral thalamus, K) with the lateral ventricle (LV), culminating ventrally by the internal capsule (L). GFP cells and processes can be seen in the periaqueductal gray (M) and ipsilateral internal capsule (N).  $\mu\text{m}$  bar is  $30\ \mu\text{m}$  in K–N.

longer transplant survival times (5 months) hESC-derived hNSC transplants differentiated 18–38% into neurons, 13–16% into astrocytes, and 11–13% into oligodendrocytes.<sup>65</sup> Alternatively, the location of the transplant could affect their potential, and studies are in progress to gather evidence to test this hypothesis. The down-regulation of neural stemness markers such as nestin and cell proliferation marker nuclear Ki67 is consistent with the observed neuronal differentiation. The diminishing of nuclear Ki-67 immunoreactivity has been reported earlier with these cells in a spinal cord injury model.<sup>72</sup> The distribution of the transplanted GFP cells and axonal processes suggests that they respond to the PBBI milieu, reminiscent of human amniotic membrane placental stem cells (AMPs) in this model. The NSI-566 cells are known to secrete neuroprotective factors such as insulin-like growth factor (IGF)-1.<sup>87</sup> Therefore, hNSCs and AMPs could mitigate PBBI-induced remote axonal damage via similar mechanisms.<sup>26,31,32</sup> Further, extension of transplant processes along existing host white matter tracts indicates the ability to recapitulate host neural pathways. Extensions through the internal capsule adjacent to the lesion into the host spinal cord suggest that these axons follow motor system pathways, which are usually disrupted in the PBBI model. In addition, presence of GFP processes in the hippocampus suggests that the transplanted cells have potential to interact with memory and learning pathways, which are known to be impaired in PBBI.<sup>26</sup> Unlike AMPs that did not need immunosuppression and were not expected to integrate, hNSCs require immunosuppression for engraftment and to differentiate into neurons in the rat host. The three-dimensional environment provided by type I collagen scaffold seemed to be required for AMP cell survival in the injury core,<sup>26</sup> whereas the hNSCs survived without any scaffold up to the latest time point tested, that is, 16 weeks post-transplantation. Similar to AMPs, a small fraction of hNSC cells migrated into the sub-ventricular zone and the corpus callosum. The fetal spinal cord-derived hNSCs had greater survival, engraftment, and neuronal differentiation than scaffolded adult rat hippocampal neural progenitor cells in this model.

Unlike rat adult progenitors that migrated into the surrounding brain and differentiated into phenotypes including astrocytes and oligodendrocytes,<sup>88</sup> hNSCs did not differentiate into non-neuronal lineages. Further, hNSCs did not need additional factors such as the soluble Nogo receptor (sNgR) to integrate with surrounding viable PBBI tissue. In this model, substantial axon formation was detected with NSI-566 hNSCs, but not with adult rat hippocampal progenitors.<sup>89</sup> Taken together, these studies suggest that with delayed transplantation with adequate immunosuppression, the PBBI milieu is conducive to hNSC engraftment.

Transplantation of viable fetal neural progenitor cells (as early as 24 h post-TBI) attenuated host neuronal degeneration (as assessed on day 6 post-transplantation), and also guided host microglia/macrophages toward an anti-inflammation phenotype, indicating a potentially beneficial effect of progenitor cell transplantation on adjacent host cells.<sup>43,47,52,53</sup> A similar mechanism needs to be investigated in this model with these cells.

In other TBI and stroke models, cells have been delivered *via* intravenous (IV), intra-arterial carotid (IAC), or intraparenchymal (IP) injections. However, IV administration causes loss of the majority (~95%) of the cells during lung passage,<sup>48,63,64,84,90</sup> whereas IAC injection carries the risk of causing embolic brain infarction and fails to deliver sufficient cells across the vascular wall barrier to the brain parenchyma, which is the major barrier for putative clinical use of this route. Engraftment after IAC injection is also dependent on cell type and adhesion molecule expression. IAC has been developed with bone marrow MSCs into a clinical trial for stroke.<sup>91,92</sup> However, in all TBI studies exploring human cell therapies with neural or non-neural origin hNSCs/progenitors, no engraftment has yet been detected with either IV or IAC.<sup>56,64,89,93</sup> Especially in PBBI, where vascular damage is characterized by hemorrhage and reduced perfusion to the lesion,<sup>27,28,78,94</sup> vascular approaches may be technically challenging. Together, these data show that direct transplantation of hNSCs to replace damaged neural networks may be a viable approach in the treatment of severe TBI.

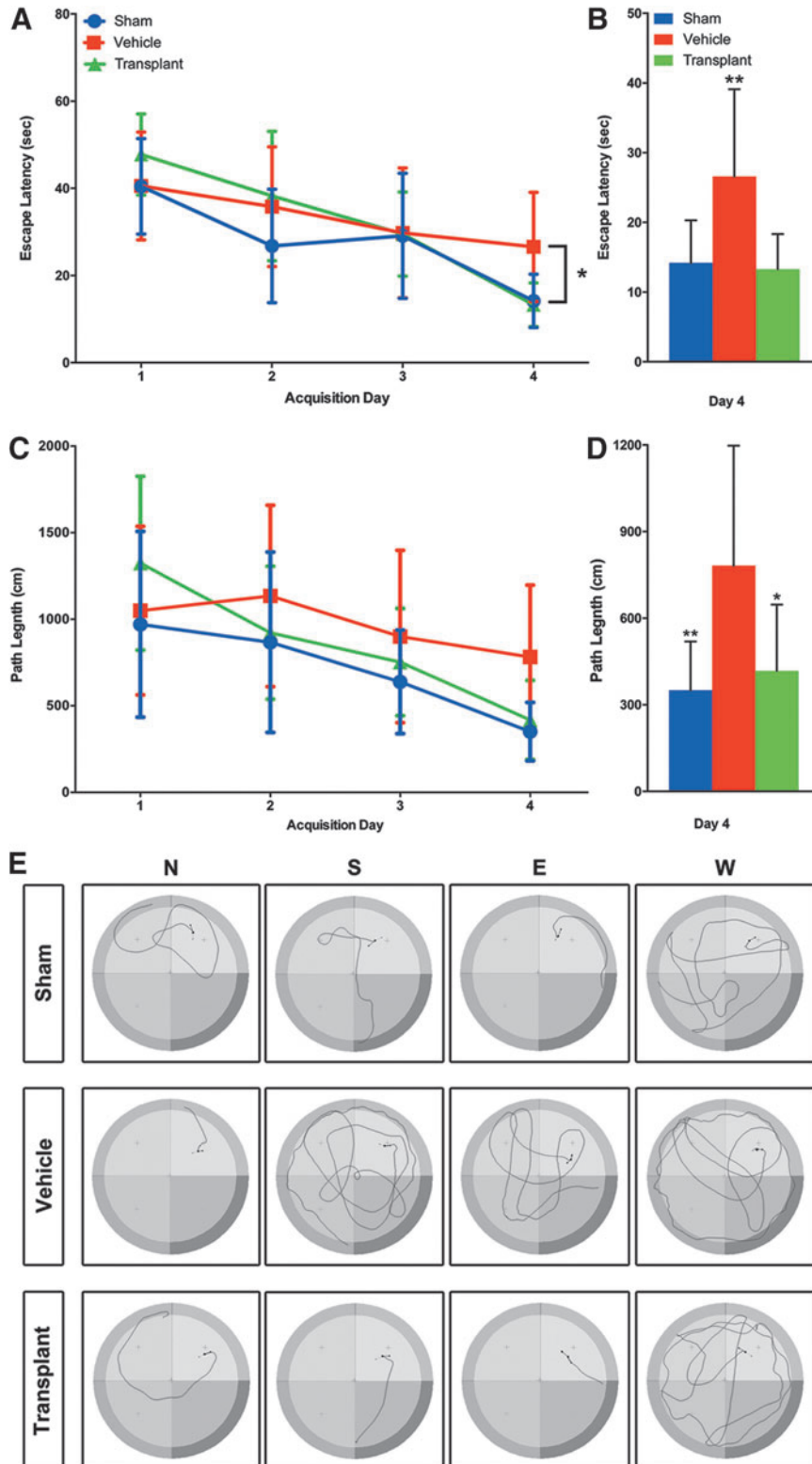
Longitudinal characterization of enduring cognitive deficits in PBBI is well documented.<sup>77</sup> Amelioration of injury-induced cognitive deficits following human cell transplantation has been extensively reviewed recently.<sup>84</sup> These studies have quantified long-term cell survival and neuronal differentiation,<sup>59,64</sup> or measured cognitive outcomes,<sup>26,31</sup> but not both. The few studies that reported cognitive benefit of human neural stem cell therapy did not exceed 8 weeks;<sup>84</sup> therefore, the time required to allow for neuronal differentiation could not demonstrate lasting benefits. In this study, the MWM revealed a PBBI effect, albeit to a lesser extent, consistent with previous work,<sup>77,95</sup> and its amelioration at 8 weeks post-transplantation was coincident with neuronal differentiation of hNSCs. The vehicle-treated PBBI animals' learning plateaued (injury effect), whereas that of transplanted PBBI animals continued to improve (reversal of injury effect). These results were both surprising and disappointing, and may be the result of a number of factors. In the absence of significant MWM deficits, we cannot state that we observed significant therapeutic benefits. However, hNSCs did no harm. The animals that received cell transplants did not perform any worse than the PBBI+vehicle

**FIG. 7.** (A) The mean latency  $\pm$  standard deviation for Morris Water Maze (MWM) behavioral outcome 8 weeks following transplantation reveals the beneficial effect of transplantation. Results across four acquisition days are compared between sham (no penetrating ballistic-like brain injury [PBBI], no cells), vehicle (PBBI, no cells), and transplant (PBBI, cell transplant) groups. Non-uniform latency to platform can be seen in all experimental groups from day 1 to day 4 of testing. By day 4, latency to reach platform was significantly lower in the sham group (blue) than in the vehicle group (red) ( $p < 0.01$ ). Latency to reach the platform was also lower in the transplant (green) group than in the vehicle group ( $p < 0.05$ ). Latency was not significantly different between the transplant and sham groups on any of the test days. There were no significant differences in latency on days 1–3 between any groups. The sham group reduced latency significantly from day 1 to day 2 and from day 3 to day 4 ( $p < 0.01$ ). Vehicle group did not reduce latency significantly between concurrent days, but improved from day 1 to day 3 ( $p < 0.05$ ). The transplant group reduced latency significantly across each concurrent day of testing (D1->D2->D3->D4,  $p < 0.05$  each) (A). A one way analysis of variance (ANOVA) for just the acquisition day 4 data revealed significant differences between sham and PBBI+ vehicle or PBBI+vehicle and PBBI+transplant (\*\* $p < 0.001$ ) (B). Path lengths did not differ significantly on a two way ANOVA (C). One way ANOVA of just the acquisition day 4 path length was significant for sham (blue) versus vehicle (red) (\*\* $p < 0.001$ ) as well as vehicle (red) versus transplant (green) (\* $p < 0.05$ ) (D). The path length tracings of a representative animal of each group from four release points (North = N, South = S, East = E, West = W) are shown in E.

group, and showed a trend on day 4 toward performing better. Taken together the data support the conclusion that there is a beneficial, but not a therapeutic, effect of transplant at 8 weeks post-transplantation. As repeated testing of the same animals abrogates the differences between groups,<sup>77</sup> future behavioral assessments at different times in separate groups can establish a time dependency of the transplant effect, and determine whether

using a working memory testing paradigm would provide more injury-sensitive results for delayed testing.

To enable replication and standardization, we suggested use of quality criteria and rigor. The effect size of PBBI (difference in mean latency to platform between sham and PBBI +vehicle/standard deviation) in this study is comparable with that published for PBBI,<sup>77</sup> and the effect size of cell therapy benefit is also



comparable with other studies with rat or human NSC transplants.<sup>47,59</sup> To our knowledge, this is the first study of human fetal neural stem cell transplant in an immunosuppressed TBI model with a duration of 16 weeks for histology, reporting robust engraftment and neuronal differentiation as well as amelioration of injury-induced cognitive impairment at 8 weeks. According to “The International Society for Stem Cell Research and Center for Biologics Evaluation and Research/Office of Cellular, Tissue and Gene Therapies”<sup>67</sup> FDA guidelines, translation of cell transplantation approach in TBI requires evidence supporting: 1) lack of hNSCs tumorigenicity in TBI models, 2) cell dose dependence of behavior alterations in TBI, 3) best site and time for transplantation after TBI, and 4) establishing feasibility and scalability of the approach to both normal and TBI animals with longer gyrencephalic brains, such as the pig or primate.<sup>66,67,96</sup> We have, therefore, embarked on a program of dose refinement and safety testing for these cells, as a prelude to human severe TBI clinical trials. Previous human NSC transplants have been shown to be safe.<sup>64</sup>

## Conclusion

This study demonstrates durable engraftment and increasing neuronal differentiation with time for hNSCs in PBBI. The immunohistochemical analysis reveals transition of proliferating hNSCs into differentiated neurons accompanied by homologous morphological changes between 8 and 16 weeks post-transplantation. Presence of presynaptic structural protein in transplant cells suggests that behavior modification is attributable to integration into host tissue. The relatively weak injury effect at the delayed time point confounds the benefits of durable engraftment and neuronal differentiation. Whether the development of these interactions between transplant and host can be evaluated by electrophysiological means needs to be determined. Nevertheless, the propensity for these cells to develop neuronal phenotype, to project extensive processes into the host brain, and to express structural components of synapse, with coincident absence of a harmful effect on cognitive deficits provides rational and feasibility data for further studies exploring the translatability of the cell therapy.

## Acknowledgments

These studies were supported in part by W81XWH-16-2-0008-BAA-150111 to R.M.B. and by the Department of Health State of Florida General Revenue Funds to The Miami Project to Cure Paralysis. P.N.S., a student volunteer from San Francisco State University (SFSU), was supported by an NIH Morehouse College Minority Biomedical Research Support – Research Initiative for Scientific Enhancement (MBRS-RISE) Fellowship and in part by an NIH Summer Student Fellowship. The authors thank Dr. Khadil Hosein, Dr. Meghan O Blaya, Dr. Lai Yee Leung, Dr. Ying Deng-Bryant, Dr. Stanislava Jergova, Dr. Melissa Carballosa-Gautam, Dr. Guobin Zhang, Dr. Adaikkalamsamy David (Titus), Dr. Philip Ruiz, Dr. Alex Marcillo, Dr. Donna Avison, David Joel Sequeira, Yoelvis Hernandez, Jessica Monterrosa Mena, Nuan Song, Matthew Aguirre, and Julia Janecki for technical contributions to this study, and Nathan Bryant Schoen, Dr. Meghan O Blaya, and Maria Muniz for proofreading the manuscript.

## Author Disclosure Statement

MPH, TGH, and KKJ are employees of Neuralstem, Inc. All other authors have no competing interests to declare.

## References

- Hyder, A.A., Wunderlich, C.A., Puvanachandra, P., Gururaj, G., and Kobusingye, O.C. (2007). The impact of traumatic brain injuries: a global perspective. *NeuroRehabilitation* 22, 341–353.
- Gold, E.M., Su, D., Lopez-Velazquez, L., Haus, D.L., Perez, H., Lacuesta, G.A., Anderson, A.J., and Cummings, B.J. (2013). Functional assessment of long-term deficits in rodent models of traumatic brain injury. *Regen. Med.* 8, 483–516.
- Tasigiorgos, S., Economopoulos, K.P., Winfield, R.D., and Sakran, J.V. (2015). Firearm injury in the United States: an overview of an evolving public health problem. *J. Am. Coll. Surg.* 221, 1005–1014.
- Joseph, B., Aziz, H., Pandit, V., Kulvatunyou, N., O’Keefe, T., Wynne, J., Tang, A., Friese, R.S., and Rhee, P. (2014). Improving survival rates after civilian gunshot wounds to the brain. *J. Am. Coll. Surg.* 218, 58–65.
- Lin, D.J., Lam, F.C., Siracuse, J.J., Thomas, A., and Kasper, E.M. (2012). “Time is brain” the Gifford factor – or: Why do some civilian gunshot wounds to the head do unexpectedly well? A case series with outcomes analysis and a management guide. *Surg. Neurol. Int.* 3, 98.
- Young, N.H., and Andrews, P.J. (2008). Developing a prognostic model for traumatic brain injury—a missed opportunity? *PLoS medicine* 5, e168.
- Corrigan, J.D., Selassie, A.W., and Orman, J.A. (2010). The epidemiology of traumatic brain injury. *J. Head Trauma Rehabil.* 25, 72–80.
- Faul M., Xu, L., Wald, M.M., Coronado, V.G. (2010). *Traumatic Brain Injury in the United States: Emergency Department Visits, Hospitalizations, and Deaths*. Centers for Disease Control and Prevention, National Center for Injury Prevention and Control: Atlanta.
- Gressot, L.V., Chamoun, R.B., Patel, A.J., Valadka, A.B., Suki, D., Robertson, C.S., and Gopinath, S.P. (2014). Predictors of outcome in civilians with gunshot wounds to the head upon presentation. *J. Neurosurg.* 121, 645–652.
- Jena, A.B., Sun, E.C., and Prasad, V. (2014). Does the declining lethality of gunshot injuries mask a rising epidemic of gun violence in the United States? *J. Gen. Intern. Med.* 29, 1065–1069.
- Langlois, J.A., Rutland-Brown, W., and Wald, M.M. (2006). The epidemiology and impact of traumatic brain injury: a brief overview. *J. Head Trauma Rehabil.* 21, 375–378.
- Rosenfeld, J.V., Bell, R.S., and Armonda, R. (2015). Current concepts in penetrating and blast injury to the central nervous system. *World J. Surg.* 39, 1352–1362.
- Defense and Veterans Brain Injury Center, Department of Defense (2016). *DoD Worldwide Numbers for TBI*. Defense and Veterans Brain Injury Center, Silver Spring, Maryland.
- Khan, M.B., Kumar, R., Irfan, F.B., Irfan, A.B., and Bari, M.E. (2014). Civilian craniocerebral gunshot injuries in a developing country: presentation, injury characteristics, prognostic indicators, and complications. *World Neurosurg.* 82, 14–19.
- Pruitt, B. (2001). Part 2: Prognosis in penetrating brain injury. *J. Trauma* 51, S44–86.
- Guevara, A.B., Demonet, J.F., Polejaeva, E., Knutson, K.M., Wassermann, E.M., Grafman, J., and Krueger, F. (2016). Association between traumatic brain injury-related brain lesions and long-term caregiver burden. *J. Head Trauma Rehabil.* 31, E48–58.
- Winn, H.R. (2011). *Youmans Neurological Surgery*, 4-Volume Set, 6th ed. Elsevier: New York.
- Streib, E., Blake, D., Christmas, A.B., Clancy, K., Cocanour, C., Cooper, C., Driscoll, R.P., Eastman, A.L., Ekeh, A.P., Gonzalez, R., Hinsdale, J.G., Joseph, K., Kuhls, D.A., Thomas, S.G., Cooper, Z., and AAST Prevention Committee (2016). American Association for the Surgery of Trauma statement on firearm injuries. *J. Trauma Acute Care Surg.* 80, 849.
- Bramlett, H.M., and Dietrich, W.D. (2002). Quantitative structural changes in white and gray matter 1 year following traumatic brain injury in rats. *Acta Neuropathol.* 103, 607–614.
- Kemie, S.G., and Parent, J.M. (2010). Forebrain neurogenesis after focal ischemic and traumatic brain injury. *Neurobiol. Dis.* 37, 267–274.
- Richardson, R.M., Sun, D., and Bullock, M.R. (2007). Neurogenesis after traumatic brain injury. *Neurosurg. Clin. N. Am.* 18, 169–181, xi.
- Lozano, D., Gonzales-Portillo, G.S., Acosta, S., de la Pena, I., Tajiri, N., Kaneko, Y., and Borlongan, C.V. (2015). Neuroinflammatory responses to traumatic brain injury: etiology, clinical consequences, and therapeutic opportunities. *Neuropsychiatr. Dis. Treat.* 11, 97–106.

23. Maxwell, W.L., MacKinnon, M.A., Stewart, J.E., and Graham, D.I. (2010). Stereology of cerebral cortex after traumatic brain injury matched to the Glasgow outcome score. *Brain* 133, 139–160.
24. Ramlackhansingh, A.F., Brooks, D.J., Greenwood, R.J., Bose, S.K., Turkheimer, F.E., Kinnunen, K.M., Gentleman, S., Heckemann, R.A., Gunanayagam, K., Gelosa, G., and Sharp, D.J. (2011). Inflammation after trauma: microglial activation and traumatic brain injury. *Ann. Neurol.* 70, 374–383.
25. Oehmichen, M., and Meissner, C. (2009). Routine techniques in forensic neuropathology as demonstrated by gunshot injury to the head. *Leg. Med.* 11, Suppl. 1, S50–53.
26. Chen, Z., Lu, X.C., Shear, D.A., Dave, J.R., Davis, A.R., Evangelista, C.A., Duffy, D., and Tortella, F.C. (2011). Synergism of human amnion-derived multipotent progenitor (AMP) cells and a collagen scaffold in promoting brain wound recovery: pre-clinical studies in an experimental model of penetrating ballistic-like brain injury. *Brain Res.* 1368, 71–81.
27. Williams, A.J., Hartings, J.A., Lu, X.C., Rolli, M.L., Dave, J.R., and Tortella, F.C. (2005). Characterization of a new rat model of penetrating ballistic brain injury. *J. Neurotrauma* 22, 313–331.
28. Williams, A.J., Wei, H.H., Dave, J.R., and Tortella, F.C. (2007). Acute and delayed neuroinflammatory response following experimental penetrating ballistic brain injury in the rat. *J. Neuroinflammation* 4, 17.
29. Lu, X.C., Shear, D.A., Graham, P.B., Bridson, G.W., Uttamsingh, V., Chen, Z., Leung, L.Y., and Tortella, F.C. (2015). Dual therapeutic effects of C-10068, a dexamethorphan derivative, against post-traumatic nonconvulsive seizures and neuroinflammation in a rat model of penetrating ballistic-like brain injury. *J. Neurotrauma*
30. Shear, D.A., and Tortella, F.C. (2013). A military-centered approach to neuroprotection for traumatic brain injury. *Front. Neurol.* 4, 73.
31. Chen, Z., Tortella, F.C., Dave, J.R., Marshall, V.S., Clarke, D.L., Sing, G., Du, F., and Lu, X.C. (2009). Human amnion-derived multipotent progenitor cell treatment alleviates traumatic brain injury-induced axonal degeneration. *J. Neurotrauma* 26, 1987–1997.
32. Deng-Bryant, Y., Readnower, R.D., Leung, L.Y., Cunningham, T.L., Shear, D.A., and Tortella, F.C. (2015). Treatment with amnion-derived cellular cytokine solution (ACCS) induces persistent motor improvement and ameliorates neuroinflammation in a rat model of penetrating ballistic-like brain injury. *Restor. Neurol. Neurosci.* 33, 189–203.
33. Bonaventura, G., Chamayou, S., Liprino, A., Guglielmino, A., Fichera, M., Caruso, M., and Barcellona, M.L. (2015). Different tissue-derived stem cells: a comparison of neural differentiation capability. *PLoS one* 10, e0140790.
34. Yan, Z.J., Zhang, P., Hu, Y.Q., Zhang, H.T., Hong, S.Q., Zhou, H.L., Zhang, M.Y., and Xu, R.X. (2013). Neural stem-like cells derived from human amnion tissue are effective in treating traumatic brain injury in rat. *Neurochem. Res.* 38, 1022–1033.
35. Kopen, G.C., Prockop, D.J., and Phinney, D.G. (1999). Marrow stromal cells migrate throughout forebrain and cerebellum, and they differentiate into astrocytes after injection into neonatal mouse brains. *Proc. Natl. Acad. Sci. U. S. A.* 96, 10711–10716.
36. Peng, W., Sun, J., Sheng, C., Wang, Z., Wang, Y., Zhang, C., and Fan, R. (2015). Systematic review and meta-analysis of efficacy of mesenchymal stem cells on locomotor recovery in animal models of traumatic brain injury. *Stem Cell Res. Ther.* 6, 47.
37. Xiong, Y., Mahmood, A., and Chopp, M. (2010). Neurorestorative treatments for traumatic brain injury. *Discov. Med.* 10, 434–442.
38. Zhang, Y., Chopp, M., Meng, Y., Katakowski, M., Xin, H., Mahmood, A., and Xiong, Y. (2015). Effect of exosomes derived from multipotent mesenchymal stromal cells on functional recovery and neurovascular plasticity in rats after traumatic brain injury. *J. Neurosurg.* 122, 856–867.
39. Steinbeck, J.A., and Studer, L. (2015). Moving stem cells to the clinic: potential and limitations for brain repair. *Neuron* 86, 187–206.
40. Rolfe, A., and Sun, D. (2015). Stem cell therapy in brain trauma: implications for repair and regeneration of injured brain in experimental TBI models, in: *Brain Neurotrauma: Molecular, Neuropsychological, and Rehabilitation Aspects*. F.H. Kobeissy (ed.). CRC Press, Boca Raton, FL, pp. 587–596.
41. Kochanek, P.M., Jackson, T.C., Ferguson, N.M., Carlson, S.W., Simon, D.W., Brockman, E.C., Ji, J., Bayir, H., Poloyac, S.M., Wagner, A.K., Kline, A.E., Empey, P.E., Clark, R.S., Jackson, E.K., and Dixon, C.E. (2015). Emerging therapies in traumatic brain injury. *Semin. Neurol.* 35, 83–100.
42. Gennai, S., Monsel, A., Hao, Q., Liu, J., Gudapati, V., Barbier, E.L., and Lee, J.W. (2015). Cell-based therapy for traumatic brain injury. *Br. J. Anaesth.* 115, 203–212.
43. Gao, J., Grill, R.J., Dunn, T.J., Bedi, S., Labastida, J.A., Hetz, R.A., Xue, H., Thonhoff, J.R., DeWitt, D.S., Prough, D.S., Cox, C.S., Jr., and Wu, P. (2016). Human neural stem cell transplantation-mediated alteration of microglial/macrophage phenotypes after traumatic brain injury. *Cell Transplant.* 25, 1863–1877.
44. Gage, F.H., and Temple, S. (2013). Neural stem cells: generating and regenerating the brain. *Neuron* 80, 588–601.
45. Anderson, A.J., Haus, D.L., Hooshmand, M.J., Perez, H., Sontag, C.J., and Cummings, B.J. (2011). Achieving stable human stem cell engraftment and survival in the CNS: is the future of regenerative medicine immunodeficient? *Regen. Med.* 6, 367–406.
46. Giusto, E., Donega, M., Cossetti, C., and Pluchino, S. (2014). Neuro-immune interactions of neural stem cell transplants: from animal disease models to human trials. *Exp. Neurol.* 260, 19–32.
47. Blaya, M.O., Tsoulfas, P., Bramlett, H.M., and Dietrich, W.D. (2015). Neural progenitor cell transplantation promotes neuroprotection, enhances hippocampal neurogenesis, and improves cognitive outcomes after traumatic brain injury. *Exp. Neurol.* 264, 67–81.
48. Harting, M.T., Sloan, L.E., Jimenez, F., Baumgartner, J., and Cox, C.S., Jr. (2009). Subacute neural stem cell therapy for traumatic brain injury. *J. Surg. Res.* 153, 188–194.
49. Ma, H., Yu, B., Kong, L., Zhang, Y., and Shi, Y. (2011). Transplantation of neural stem cells enhances expression of synaptic protein and promotes functional recovery in a rat model of traumatic brain injury. *Mol. Med. Rep.* 4, 849–856.
50. Ma, H., Yu, B., Kong, L., Zhang, Y., and Shi, Y. (2012). Neural stem cells over-expressing brain-derived neurotrophic factor (BDNF) stimulate synaptic protein expression and promote functional recovery following transplantation in rat model of traumatic brain injury. *Neurochem. Res.* 37, 69–83.
51. Al Nimer, F., Wennersten, A., Holmin, S., Meijer, X., Wahlberg, L., and Mathiesen, T. (2004). MHC expression after human neural stem cell transplantation to brain contused rats. *Neuroreport* 15, 1871–1875.
52. Gao, J., Prough, D.S., McAdoo, D.J., Grady, J.J., Parsley, M.O., Ma, L., Tarensenko, Y.I., and Wu, P. (2006). Transplantation of primed human fetal neural stem cells improves cognitive function in rats after traumatic brain injury. *Exp. Neurol.* 201, 281–292.
53. Hagan, M., Wennersten, A., Meijer, X., Holmin, S., Wahlberg, L., and Mathiesen, T. (2003). Neuroprotection by human neural progenitor cells after experimental contusion in rats. *Neurosci. Lett.* 351, 149–152.
54. Hwang do, W., Jin, Y., Lee do, H., Kim, H.Y., Cho, H.N., Chung, H.J., Park, Y., Youn, H., Lee, S.J., Lee, H.J., Kim, S.U., Wang, K.C., and Lee, D.S. (2014). In vivo bioluminescence imaging for prolonged survival of transplanted human neural stem cells using 3D biocompatible scaffold in corticectomized rat model. *PLoS One* 9, e105129.
55. Lee, D.H., Lee, J.Y., Oh, B.M., Phi, J.H., Kim, S.K., Bang, M.S., Kim, S.U., and Wang, K.C. (2013). Functional recovery after injury of motor cortex in rats: effects of rehabilitation and stem cell transplantation in a traumatic brain injury model of cortical resection. *Child Nerv. Syst.* 29, 403–411.
56. Lundberg, J., Sodersten, E., Sundstrom, E., Le Blanc, K., Andersson, T., Hermanson, O., and Holmin, S. (2012). Targeted intra-arterial transplantation of stem cells to the injured CNS is more effective than intravenous administration: engraftment is dependent on cell type and adhesion molecule expression. *Cell Transplant.* 21, 333–343.
57. Skardelly, M., Gaber, K., Burdack, S., Scheidt, F., Schuhmann, M.U., Hilbig, H., Meixensberger, J., and Boltze, J. (2014). Transient but not permanent benefit of neuronal progenitor cell therapy after traumatic brain injury: potential causes and translational consequences. *Front. Cell. Neurosci.* 8, 318.
58. Wang, E., Gao, J., Yang, Q., Parsley, M.O., Dunn, T.J., Zhang, L., DeWitt, D.S., Denner, L., Prough, D.S., and Wu, P. (2012). Molecular mechanisms underlying effects of neural stem cells against traumatic axonal injury. *J. Neurotrauma* 29, 295–312.
59. Wennersten, A., Holmin, S., Al Nimer, F., Meijer, X., Wahlberg, L.U., and Mathiesen, T. (2006). Sustained survival of xenografted human neural stem/progenitor cells in experimental brain trauma despite discontinuation of immunosuppression. *Exp. Neurol.* 199, 339–347.

60. Wennersten, A., Meier, X., Holmin, S., Wahlberg, L., and Mathiesen, T. (2004). Proliferation, migration, and differentiation of human neural stem/progenitor cells after transplantation into a rat model of traumatic brain injury. *J. Neurosurg.* 100, 88–96.
61. Tsyb, A.F., Yuzhakov, V.V., Roshal, L.M., Sukhikh, G.T., Konoplyannikov, A.G., Sushkevich, G.N., Yakovleva, N.D., Ingel, I.E., Bandurko, L.N., Sevankava, L.E., Mikhina, L.N., Fomina, N.K., Marci, M.V., Semenova Zh, B., Konoplyannikova, O.A., Kal'sina, S., Lepekina, L.A., Semenkova, I.V., Agaeva, E.V., Shevchuk, A.S., Pavlova, L.N., Tokarev, O.Y., Karaseva, O.V., and Chernyshova, T.A. (2009). Morphofunctional study of the therapeutic efficacy of human mesenchymal and neural stem cells in rats with diffuse brain injury. *Bull. Exp. Biol. Med.* 147, 132–146.
62. Roshal, L.M., Tzyb, A.F., Pavlova, L.N., Soushevitch, G.N., Semenova, J.B., Javoronkov, L.P., Kolganova, O.I., Konoplyannikov, A.G., Shevchuk, A.S., Yujakov, V.V., Karaseva, O.V., Ivanova, T.F., Chernyshova, T.A., Konoplyannikova, O.A., Bandurko, L.N., Marey, M.V., and Sukhikh, G.T. (2009). Effect of cell therapy on recovery of cognitive functions in rats during the delayed period after brain injury. *Bull. Exp. Biol. Med.* 148, 140–147.
63. Ahmed, A.I., Gajavelli, S., Spurlock, M.S., Chieng, L.O., and Bullock, M.R. (2015). Stem cells for therapy in TBI. *J. R. Army Med. Corps* 162, 98–102.
64. Skardelly, M., Gaber, K., Burdack, S., Scheidt, F., Hilbig, H., Boltze, J., Forschler, A., Schwarz, S., Schwarz, J., Meixensberger, J., and Schuhmann, M.U. (2011). Long-term benefit of human fetal neuronal progenitor cell transplantation in a clinically adapted model after traumatic brain injury. *J. Neurotrauma* 28, 401–414.
65. Haus, D.L., Lopez-Velazquez, L., Gold, E.M., Cunningham, K.M., Perez, H., Anderson, A.J., and Cummings, B.J. (2016). Transplantation of human neural stem cells restores cognition in an immunodeficient rodent model of traumatic brain injury. *Exp. Neurol.* 281, 1–16.
66. Bailey, A.M., Mendicino, M., and Au, P. (2014). An FDA perspective on preclinical development of cell-based regenerative medicine products. *Nat. Biotechnol.* 32, 721–723.
67. Office of Cellular, Tissue, and Gene Therapy (OCTGT). (2013). *Guidance for Industry Preclinical Assessment of Investigational Cellular and Gene Therapy Products*. Services, U.S. Food and Drug Administration: Silver Spring, MD.
68. Guo, X., Johe, K., Molnar, P., Davis, H., and Hickman, J. (2010). Characterization of a human fetal spinal cord stem cell line, NSI-566RSC, and its induction to functional motoneurons. *J. Tissue Eng. Regen. Med.* 4, 181–193.
69. Feldman, E.L., Boulis, N.M., Hur, J., Johe, K., Rutkove, S.B., Federici, T., Polak, M., Bordeau, J., Sakowski, S.A., and Glass, J.D. (2014). Intraspinous neural stem cell transplantation in amyotrophic lateral sclerosis: phase I trial outcomes. *Ann. Neurol.* 75, 363–373.
70. Glass, J.D., Boulis, N.M., Johe, K., Rutkove, S.B., Federici, T., Polak, M., Kelly, C., and Feldman, E.L. (2012). Lumbar intraspinal injection of neural stem cells in patients with amyotrophic lateral sclerosis: results of a phase I trial in 12 patients. *Stem Cells* 30, 1144–1151.
71. Hefferan, M.P., Galik, J., Kakinohana, O., Sekerkova, G., Santucci, C., Marsala, S., Navarro, R., Hruska-Plochan, M., Johe, K., Feldman, E., Cleveland, D.W., and Marsala, M. (2012). Human neural stem cell replacement therapy for amyotrophic lateral sclerosis by spinal transplantation. *PLoS One* 7, e42614.
72. Lu, P., Wang, Y., Graham, L., McHale, K., Gao, M., Wu, D., Brock, J., Blesch, A., Rosenzweig, E.S., Havton, L.A., Zheng, B., Conner, J.M., Marsala, M., and Tuszynski, M.H. (2012). Long-distance growth and connectivity of neural stem cells after severe spinal cord injury. *Cell* 150, 1264–1273.
73. Riley, J., Federici, T., Polak, M., Kelly, C., Glass, J., Raore, B., Taub, J., Kesner, V., Feldman, E.L., and Boulis, N.M. (2012). Intraspinous stem cell transplantation in amyotrophic lateral sclerosis: a phase I safety trial, technical note, and lumbar safety outcomes. *Neurosurgery* 71, 405–416.
74. Riley, J., Glass, J., Feldman, E.L., Polak, M., Bordeau, J., Federici, T., Johe, K., and Boulis, N.M. (2014). Intraspinous stem cell transplantation in amyotrophic lateral sclerosis: a phase I trial, cervical microinjection, and final surgical safety outcomes. *Neurosurgery* 74, 77–87.
75. Tadesse, T., Gearing, M., Senitzer, D., Saxe, D., Brat, D.J., Bray, R., Gebel, H., Hill, C., Boulis, N., Riley, J., Feldman, E., Johe, K., Hazel, T., Polak, M., Bordeau, J., Federici, T., and Glass, J.D. (2014). Analysis of graft survival in a trial of stem cell transplant in ALS. *Ann. Clin. Transl. Neurol.* 1, 900–908.
76. Tajiri, N., Quach, D.M., Kaneko, Y., Wu, S., Lee, D., Lam, T., Hayama, K.L., Hazel, T.G., Johe, K., Wu, M.C., and Borlongan, C.V. (2014). Behavioral and histopathological assessment of adult ischemic rat brains after intracerebral transplantation of NSI-566RSC cell lines. *PLoS One* 9, e91408.
77. Shear, D.A., Lu, X.C., Bombard, M.C., Pedersen, R., Chen, Z., Davis, A., and Tortella, F.C. (2010). Longitudinal characterization of motor and cognitive deficits in a model of penetrating ballistic-like brain injury. *J. Neurotrauma* 27, 1911–1923.
78. Gajavelli, S., Kentaro, S., Diaz, J., Yokobori, S., Spurlock, M., Diaz, D., Jackson, C., Wick, A., Zhao, W., Leung, L.Y., Shear, D., Tortella, F., and Bullock, M.R. (2015). Glucose and oxygen metabolism after penetrating ballistic-like brain injury. *J. Cereb. Blood Flow Metabol.* 35, 773–780.
79. Hefferan, M.P., Johe, K., Hazel, T., Feldman, E.L., Lunn, J.S., and Marsala, M. (2011). Optimization of immunosuppressive therapy for spinal grafting of human spinal stem cells in a rat model of ALS. *Cell Transplant.* 20, 1153–1161.
80. Yan, J., Xu, L., Welsh, A.M., Chen, D., Hazel, T., Johe, K., and Koliatsos, V.E. (2006). Combined immunosuppressive agents or CD4 antibodies prolong survival of human neural stem cell grafts and improve disease outcomes in amyotrophic lateral sclerosis transgenic mice. *Stem Cells* 24, 1976–1985.
81. Vorhees, C.V. and Williams, M.T. (2006). Morris water maze: procedures for assessing spatial and related forms of learning and memory. *Nat. Protoc.* 1, 848–858.
82. Cumming, G., Fidler, F., and Vaux, D.L. (2007). Error bars in experimental biology. *J. Cell Biol.* 177, 7–11.
83. Wei, H.H., Lu, X.C., Shear, D.A., Waghay, A., Yao, C., Tortella, F.C., and Dave, J.R. (2009). NNZ-2566 treatment inhibits neuroinflammation and pro-inflammatory cytokine expression induced by experimental penetrating ballistic-like brain injury in rats. *J. Neuroinflammation* 6, 19.
84. Chang, J., Phelan, M., and Cummings, B.J. (2015). A meta-analysis of efficacy in pre-clinical human stem cell therapies for traumatic brain injury. *Exp. Neurol.* 273, 225–233.
85. Tennstaedt, A., Aswendt, M., Adamczak, J., Collienne, U., Selt, M., Schneider, G., Henn, N., Schaefer, C., Lagouge, M., Wiedermann, D., Kloppenburg, P., and Hoehn, M. (2015). Human neural stem cell intracerebral grafts show spontaneous early neuronal differentiation after several weeks. *Biomaterials* 44, 143–154.
86. Wu, P., Ye, Y., and Svendsen, C.N. (2002). Transduction of human neural progenitor cells using recombinant adeno-associated viral vectors. *Gene Ther.* 9, 245–255.
87. Yan, J., Xu, L., Welsh, A.M., Hatfield, G., Hazel, T., Johe, K., and Koliatsos, V.E. (2007). Extensive neuronal differentiation of human neural stem cell grafts in adult rat spinal cord. *PLoS Med.* 4, e39.
88. Elias, P.Z., and Spector, M. (2012). Implantation of a collagen scaffold seeded with adult rat hippocampal progenitors in a rat model of penetrating brain injury. *J. Neurosci. Methods* 209, 199–211.
89. Elias, P.Z., and Spector, M. (2015). Treatment of penetrating brain injury in a rat model using collagen scaffolds incorporating soluble Nogo receptor. *J. Tissue Eng. Regen. Med.* 9, 137–150.
90. Pendharkar, A.V., Chua, J.Y., Andres, R.H., Wang, N., Gaeta, X., Wang, H., De, A., Choi, R., Chen, S., Rutt, B.K., Gambhir, S.S., and Guzman, R. (2010). Biodistribution of neural stem cells after intravascular therapy for hypoxic-ischemia. *Stroke* 41, 2064–2070.
91. Leong, W.K., Lewis, M.D., Koblar, S.A. (2013). Preclinical studies on human cell-based therapy in rodent ischemic stroke models: Where are we now after a decade? *Stem Cells* 31, 1040–1043.
92. Yavagal, D.R., Lin, B., Raval, A.P., Garza, P.S., Dong, C., Zhao, W., Rangel, E.B., McNiece, I., Rundek, T., Sacco, R.L., Perez-Pinzon, M., and Hare, J.M. (2014). Efficacy and dose-dependent safety of intra-arterial delivery of mesenchymal stem cells in a rodent stroke model. *PLoS One* 9, e93735.
93. Tajiri, N., Acosta, S.A., Shahaduzzaman, M., Ishikawa, H., Shinozuka, K., Pabon, M., Hernandez-Ontiveros, D., Kim, D.W., Metcalf, C., Staples, M., Dailey, T., Vasconcellos, J., Franyuti, G., Gould, L., Patel, N., Cooper, D., Kaneko, Y., Borlongan, C.V., and Bickford, P.C. (2014). Intravenous transplants of human adipose-derived stem cell protect the brain from traumatic brain injury-induced neurodegeneration and motor and cognitive impairments: cell graft biodistribution and soluble factors in young and aged rats. *J. Neurosci.* 34, 313–326.
94. Boute, A.M., Yao, C., Kobeissy, F., May Lu, X.C., Zhang, Z., Wang, K.K., Schmid, K., Tortella, F.C., and Dave, J.R. (2012). Proteomic

- analysis and brain-specific systems biology in a rodent model of penetrating ballistic-like brain injury. *Electrophoresis* 33, 3693–3704.
95. Dixon, C.E., Bramlett, H.M., Dietrich, W.D., Shear, D.A., Yan, H.Q., Deng-Bryant, Y., Mondello, S., Wang, K.K., Hayes, R.L., Empey, P.E., Povlishock, J.T., Tortella, F.C., and Kochanek, P.M. (2016). Cyclosporine treatment in traumatic brain injury: operation brain trauma therapy. *J. Neurotrauma* 33, 553–566.
96. Hyun, I., Lindvall, O., Ahrlund-Richter, L., Cattaneo, E., Cavazzana-Calvo, M., Cossu, G., De Luca, M., Fox, I.J., Gerstle, C., Goldstein, R.A., Hermeren, G., High, K.A., Kim, H.O., Lee, H.P., Levy-Lahad, E., Li, L., Lo, B., Marshak, D.R., McNab, A., Munsie, M., Nakauchi, H., Rao, M., Rooke, H.M., Valles, C.S., Srivastava, A., Sugarman, J., Taylor, P.L., Veiga, A., Wong, A.L., Zoloth, L., and Daley, G.Q. (2008). New ISSCR guidelines underscore major principles for responsible translational stem cell research. *Cell Stem Cell* 3, 607–609.

Address correspondence to:

*Shyam Gajavelli, PhD*

*Miami Project to Cure Paralysis*

*1095 NW 14th Terrace*

*Miami, FL 33136*

*E-mail: shyam@miami.edu*